Characterizing Effective d_{31} Values for PZT from the Nonlinear Oscillations of Clamped-Clamped Micro- Resonators

Andrew J. Dick

Rice University, Department of Mechanical Engineering and Materials Science, Nonlinear Phenomena Laboratory, USA

In order to accurately predict the performance of micro-electromechanical systems which use piezoelectric material, precise knowledge of the piezoelectric coefficients is critical. Current material characterization methods rely on either simple structures restricted to small amplitude, linear oscillations or consider the piezoelectric material separate from the specific micro-scale device. A method is proposed for the characterization of the effective transverse piezoelectric coefficient d31 of lead zirconate titanate in a clamped-clamped micro-beam resonator experiencing nonlinear oscillations. Parameter trends identified by using a parametric identification scheme are analyzed and an approach is presented to calculate the linear piezoelectric coefficient. This method utilizes the relationship between a DC bias added to the excitation signal and the frequency shift experienced by the nonlinear response behavior. Through an additional numerical study, the sensitivity of the results to changes in the device length is identified and all data sets provide the same coefficient value when a length variation of less than 2% is allowed.

Keywords: Piezoelectric material, micro-beam resonator, nonlinear oscillations

0 INTRODUCTION

Piezoelectric material is attractive for the development of a wide range of micro-electromechanical systems (MEMS). With the ability to transform strain into an electric current through the direct piezoelectric effect and, by way of the converse piezoelectric effect, convert an applied electric field into stress, piezoelectric material is used to provide both sensing and actuation capabilities. Some examples of MEMS devices which utilize piezoelectric material that have recently been developed include contour-mode micro-resonators [1], shunt-type ohmic RF MEMS switches [2], MEMS generators [3], nano-robotics [4], and three-dimensional valveless micro-pumps [5].

In the design of piezoelectric MEMS devices, it is important to know the properties of the piezoelectric material in order to accurately predict actuation and sensing performance. One of the most important properties in many MEMS devices is the transverse piezoelectric coefficient d_{31}. Due to the different methods employed in the fabrication of these devices, the effective properties of these materials may vary significantly. In order to address this issue, it is important to have methods to successfully characterize these materials. This need has led to the development of various methods for characterizing piezoelectric materials.

These studies have utilized micro-scale cantilevered structures as well as different styles of micro-scale diaphragms and membranes in the characterization of thin film piezoelectric materials. Working with these structures, the properties of the piezoelectric materials were determined by analyzing static deformations [6] to [8] and resonance frequency shifts [7] and [9]. Dynamic responses were also used to characterize piezoelectric materials, often at very low frequencies to avoid large amplitude oscillations associated with resonance and the potential nonlinear behavior which may result [9] to [12].

While these methods are effective for low amplitude oscillations, the use of linear modeling techniques, such as those employed by many finite element models, significantly limit the effective operation range of these methods. Due to the influence of scaling on these structures, their behavior has been found to become significantly nonlinear more readily than equivalent macro-scale structures [13] to [15]. When characterizing the effective properties of piezoelectric materials from the oscillations of a MEMS device, the linear range can be limiting and monitoring these "small" amplitude oscillations may require the use of high precision measurement equipment. When nonlinear properties are introduced, system dynamics can become complicated and specific nonlinear analysis techniques are required (e.g. [16]).
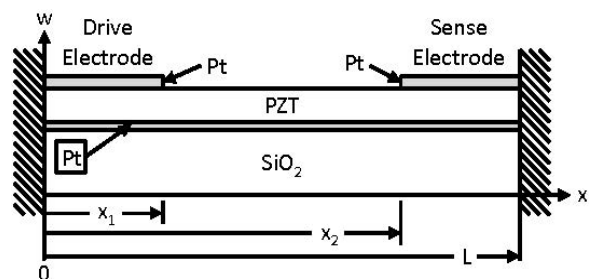

Fig. 1. *Diagram of the side view of a clamped-clamped beam resonator*

*Corr. Author's Address: Rice University, Department of Mechanical Engineering and Materials Science, 6100 Main Street, Houston, Texas, USA, andrew.j.dick@rice.edu

For excitation magnitudes above the levels which produce linear behavior, micro-scale structures can exhibit nonlinear frequency-response behavior. Nonlinear Düffing-like hard-ening behavior has been observed in frequency-response data collected from clamped-clamped style beam resonators for harmonic excitation with constant amplitude and a range of bias voltage levels. A diagram of the device config-uration is presented in Fig. 1. The drive and sense electrodes are each one-quarter of the device length to provide the best electro-mechanical coupling [17]. The frequency-response data collected from these devices can be analyzed by using a parametric identification scheme devel-oped by the author [18]. Parametric identification techniques rely on an accurate model of the system under investigation in order to calculate specific system parameters (e.g. [19]).

This parametric identification scheme is used to calculate the parameter values associated with a discretized system model from nonlinear frequency-response data. For the clamped-clamped beam-like multi-segment and multi-layered micro-structure considered, a nonlinear partial integro-differential beam equation is used. This equation, presented as Eq. (1), includes the standard terms of an Euler-Bernoulli beam model as well as a term for an applied axial force and an integral term to account for axial stretching which results from large displacements.

The segmenting of the top platinum electrode layer is modeled as three beams in series with the subscript n for $n = 1$, 2, and 3. The three sections correspond to $0 < x < x_1$, $x_1 < x < x_2$, $x_2 < x < L$. This allows for the model to accurately represent the decrease in the stiffness of the structure caused by the absence of the middle segment of the top platinum electrode and its subsequent effect on the characteristic frequencies and mode shapes.

$$\rho A_n w_{n,tt} + c_n w_{n,t} + EI_n w_{n,xxxx} -$$

$$-\sum_{m=1}^{3}\left[\frac{1}{2}\frac{EA_m}{L}\int_{x_{m-1}}^{x_m}\left(w_{m,x}\right)^2 dx\right]w_{n,xx} - P_0 w_{n,xx} = M_{n,xx}. \quad (1)$$

Subscripts following commas indicate partial derivatives. The parameters w, ρA, c, EI, EA, L, P_0, and M corresponds to the transverse displacement, mass per length, viscous damping, flexural rigidity, axial stiffness, length, axial force, and applied moment, respectively. The applied moment is produced by the axial force from the actuated piezoelectric layer and the offset between the piezoelectric layer and the neutral axis of composite structure. The values of ρA, EI, and EA are averaged across the three or four layers in each of the sections [20].

In order to complete the model, four boundary conditions and eight compatibility conditions are defined. The boundary conditions correspond to a clamped-clamped configuration. The compatibility conditions ensure that position, slope, moment, and shear force are balanced at positions x_1 and x_2.

By using linear mode shapes calculated with a linear form of Eq. (1), the boundary conditions, and the compatibility conditions, Eq. (1) is discretized with the Galerkin method to produce a single mode approximation, defined in Eq. (2). The use of the linear mode shapes is based on the assumption that the structure only exhibits weakly nonlinear behavior.

$$\bar{m}\ddot{q}_1 + \bar{c}\dot{q}_1 + k q_1 + \alpha_3 q_1^3 = F_0 \cos\left(\omega t\right). \quad (2)$$

The variables q_1, $\bar{m}$, $\bar{c}$, k, a_3, F_0, ω, and t correspond to the first mode response, modal mass, modal damping, stiffness, nonlinear stiffness, excitation magnitude, excitation frequency, and time. By using the first order approximate analytical solution to Eq. (2) calculated by using the method of multiple scales [21], the equations for an analytical frequency-response curve are derived. The assumption of weakly nonlinear behavior is also required in order to apply the method of multiple scales to Eq. (2). By tuning the parameter values in order to match the analytical frequency-response curve with the experimental data, the values of the system parameters in Eq. (2) are identified.

An additional step in this process is used to identify the value of the axial force in order to match the identified effective linear natural frequency with the frequency from an analytical model. Through an iterative process, the parameter values are identified to the desired level of precision. A complete description of the parametric identification process is presented in reference [18].

Table 1. *Resonator dimensions*

Dimension	Value
Width	20 μm
Thickness, SiO$_2$	1.06 μm
Thickness, Bottom *Pt*	135 nm
Thickness, PZT	530 nm
Thickness, Top Pt	200 nm

The remainder of the paper is organized in the following manner. The data analyzed in this study is discussed in section one. In section two, the method proposed for calculating the effective transverse piezoelectric coefficient is presented. Results obtained from the application of the proposed method are

presented in section three. Concluding remarks and comments on the direction of future work are gathered in the section four.

1 PIEZOELECTRIC MICRO-RESONATORS

The devices examined within this study consists of a silicon dioxide base layer, a bottom platinum electrode layer, a layer of sol-gel lead zirconate titanate (PZT), and a segmented top platinum electrode layer [17]. The dimensions of the devices studied are listed in Table 1. Data collected from devices with lengths of 100, 200 and 400 μm is examined.

In order to characterize the piezoelectric material in these devices, multiple data sets of frequency-response data are collected from piezoelectrically actuated clamped-clamped beam-style micro-scale devices. A sweep-sine signal with an added DC bias was applied to the drive electrodes and a laser Doppler vibrometer focused onto the center of the device was used to measure the device's response at room temperature and pressure. Bias voltage levels ranged from 0 to 4 volts corresponding to electric field strength values of up to 7.55×10^6 volts per meter were applied. Representative data collected by using this method is presented in Fig. 2. The dashed lines indicate where the response of the resonator abruptly changed from high amplitude to low amplitude responses for increasing frequency sweeps due to the nonlinear stiffening property of the structure.
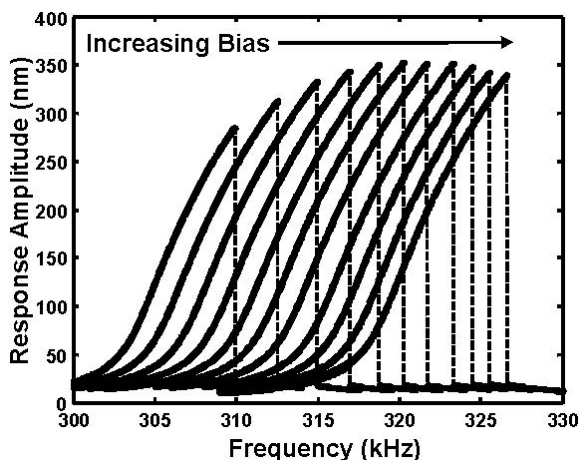

Fig. 2. *Representative nonlinear frequency-response data for a range of bias voltage levels*

2 CHARACTERIZATION METHOD

By analyzing the experimental data, the effective linear transverse piezoelectric coefficient is calculated for the sol-gel PZT, specifically the $PZ_{52}T_{48}$ used within the devices [22]. Here the method to characterize the properties of PZT in MEMS devices is presented.

The method for determining the effective transverse piezoelectric coefficient is based upon the relationship between the additional DC bias voltage added to the harmonic input signal and resulting axial force produced in the structure. However, it is not possible to measure the axial force in the micro-resonator directly. This information is determined indirectly from the effective linear natural frequency which is calculated from the identified values of the linear stiffness k and modal mass $\bar{m}$ measured with the parametric identification scheme. In order to calculate a value for the axial force versus DC bias voltage, the frequency versus axial force and frequency versus DC bias voltage are first calculated.

When examining the effective linear natural frequency versus DC bias data, the influence of the hysteretic properties of the piezoelectric material is clearly observed. This property can be seen in the representative plot of frequency versus DC bias for a 200 μm device in Fig. 3. The hysteretic characteristics of the frequency versus DC bias are addressed by fitting a linear approximation to the identified parameter values in a least-squares sense. In Fig. 3, the joined data points correspond to the identified effective linear natural frequency values for a range of DC bias voltage values. The linear approximation is represented in the figure by the dashed line. While the hysteretic properties of the response are not captured by the linear approximation, it does provide an effective representation of the general frequency-voltage relationship, especially for decreasing DC bias voltage values.
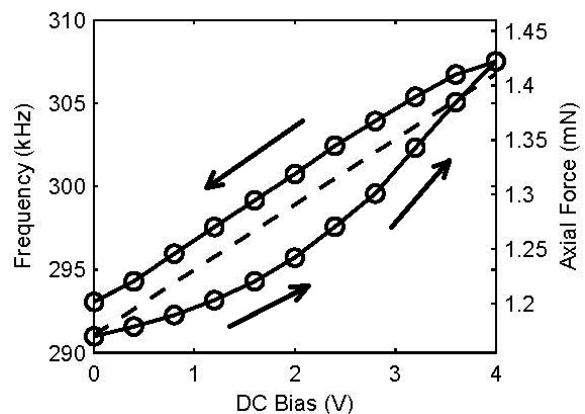

Fig. 3. *Representative plot of linear natural frequency of a 200 mm piezoelectric micro-resonator versus DC bias (joined data points) and linear approximation (dashed line)*

In order to calculate the relationship between the axial force and the effective linear natural frequency, an Euler-Bernoulli beam model with an axial force term is used, as defined by Eq. (3).

$$\rho A_n \, w_{n,tt} + EI_n \, w_{n,xxxx} - F_\Lambda \, w_{n,xx} = 0. \qquad (3)$$

The tensile axial force induced by the piezoelectric layer is represented by F_Λ. This force is defined by using the block force model in terms of the free-strain, material properties, and geometry of the layer of piezoelectric material by the formula presented in Eq. (4).

$$F_\Lambda = -E_{PZT} b_{PZT} \Lambda_{13} t_{PZT}. \qquad (4)$$

The simplification used by the block force model results in an over estimation of the predicted force. The negative sign indicates that a positive bias voltage will result in a compressive axial force under the drive electrode. The other two segments of the micro-structure are subjected to equal and opposite axial loading which results in an increase in the device's fundamental frequency. The free-strain Λ_{13} is defined in terms of the transverse piezoelectric coefficient d_{31}, the applied DC voltage VDC, and the thickness of the piezoelectric material t_{PZT}.
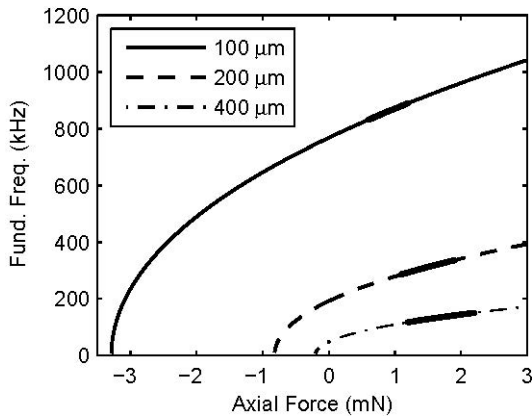

Fig. 4. *Fundamental frequency for a range of axial force values with linear trendlines (thick) over ranges of relevant frequency values*

$$\Lambda_{13} = d_{31} \left(V_{DC} / t_{PZT} \right). \qquad (5)$$

The nonlinear relationship between the fundamental frequency of the micro-structure and the applied axial load calculated by using Eq. (3) and clamped-clamped boundary conditions is illustrated in Fig. 4 for three device lengths: 100 μm (solid), 200 μm (dashed), and 400 μm (dot-dashed).

Fundamental frequency values drop to zero when the device undergoes buckling. Post-buckling conditions are not considered in this study. The high accuracy linear approximation for the relationship between the fundamental frequency and the axial force (kHz/F_Λ) and the linear approximation of the fundamental frequency with the bias voltage (kHz/V_{DC}) are used to calculate a relationship between the axial force and the bias voltage (F_Λ/V_{DC}). This information is used with Eq. (6), which is derived from Eqs. (4) and (5), to calculate a value for the transverse piezoelectric coefficient.

$$d_{31} = -\frac{F_\Lambda}{V_{DC}} \frac{1}{E_{PZT} b_{PZT}}. \qquad (6)$$

Table 2. *Fundamental frequency ranges*

Length [μm]	Min. [kHz]	Max. [kHz]
100	847	877
200	291	320
400	121	146

Table 3. *Linear approximation details*

Length [μm]	Slope [kHz/mN]	Intercept [kHz]	R^2
100	96.98	774.01	0.99999
200	62.45	218.28	0.99989
400	32.98	78.69	0.99963

3 RESULTS

By using the frequency-voltage slope values calculated from seven data sets, the frequency-force slope values listed in Table 3, and the material properties and geometry, transverse piezoelectric coefficient values are calculated. These values are listed in Table 4 along with the corresponding force-voltage information. By assuming each device is of nominal length, transverse piezoelectric coefficient values range from −119.13 to −141.52 pm/V. This corresponds to a mean value of −129.67 pm/V with a standard deviation of less than 6% of the mean. Based on the use of the block force model, these values represent an upper bounds for the transverse piezoelectric coefficient values. While the values presented in Table 4 do not suggest any trends associated with device length, the fabrication methods used generally results in undercutting which will cause the device length to deviate from the nominal value.

Although the device length does not directly affect the d_{31} value in Eq. (6), it does affect the value of the kHz/F_Λ slope. In order to study this influence, kHz/F_Λ slope values are calculated for length variations of ±7.5% for each of the three nominal

device lengths. The slope values of the linear approximations calculated over this range have R^2 values that deviate from unity by less than one-tenth of a percent. This data is plotted in Fig. 5 along with a second order polynomial fit to the data. The R^2 values for the three polynomial fits are within three-tenths of a percent of unity and provide a highly accurate representation of the relationship between the kHz/F_Λ slope and the effective device length.

Table 4. *Calculated d_{31} values*

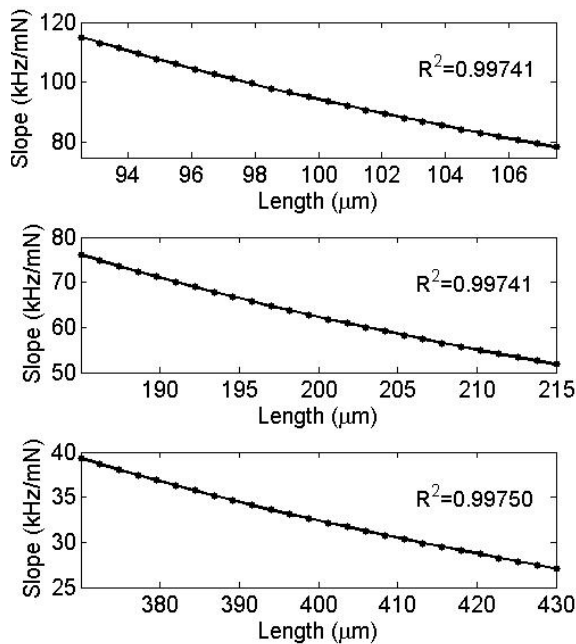| Nom. L [μm]	F_Λ/V_{DC} [$\mu N/V$]	d_{31} [pm/V]
100	70.76	−141.52
200	59.56	−119.12
200	63.21	−126.42
200	68.06	−136.12
400	62.08	−124.16
400	63.91	−127.82
400	66.26	−132.52

Fig. 5. *Calculated slope values (points) for a range of length values around the nominal values and a second order polynomial fit (curve) to the data*

By using these relationships, it is possible to explore how variations in the length will affect the calculated values of the transverse piezoelectric coefficient. The d_{31} values for all seven of the data sets are equal to −127.84 pm/V when the average length variation of less than 2%. This reveals that the value of the transverse piezoelectric is sensitive to variations in length for the clamped-clamped style

devices used. However, the values calculated are significantly greater than those of other efforts [6] to [9] and [11]. In these studies, a Young's modulus value of about 100 GPa was used for the PZT, which is significantly greater than the value used in this study. Due to the nature of Eq. (6), an increase in the value of the Young's modulus would result in a decrease in the value of the calculated transverse piezoelectric coefficient.

4 CONCLUDING REMARKS

In this study, the nonlinear oscillations of a clamped-clamped beam piezoelectric micro-scale resonator have been analyzed to calculate effective transverse piezoelectric coefficient values. By using the shift in the effective natural frequency of the nonlinear oscillator along with the analytical relationship between the axial force and this frequency, the transverse piezoelectric coefficient values have been calculated. The influence of variations in the length has been studied and the value of d_{31} has been determined to be sensitive to length. When allowing for an average length variation of less than 2%, a value of d_{31} = −127.84 pm/V for the lead zirconate titanate material in the devices from which the seven data sets were collected. The large value is attributed to the smaller value of the Young's modulus which had been identified for the devices and which has been used in this study.

5 ACKNOWLEDGEMENTS

6 REFERENCES

[1] Zuo, C., Sinha, N., Piazza, G. (2010). Very high frequency channel-select MEMS filters based on self-coupled piezoelectric AlN contour-mode resonators. *Sensors and Actuators A: Physical*, vol. 160, no. 1-2, p. 132-140, DOI:10.1016/j.sna.2010.04.011.

[2] Lee, H.-C., Park, J.-H., Park, Y.-H. (2007). Development of shunt type ohmic RF MEMS switches actuated by piezoelectric cantilever. *Sensors and Actuators A: Physical*, vol. 136, no. 1, p. 282-290, DOI:10.1016/j.sna.2006.10.050.

[3] Lee, B.S., Lin, S.C., Wu, W.J., Wang, X.Y., Chang, P.Z., Lee, C.K. (2009). Piezoelectric MEMS generators fabricated with an aerosol deposition PZT thin film.

Journal of Micromechanics and Microengineering, vol. 19, no. 6, art. no. 065014, DOI:10.1088/0960-1317/19/6/065014.

[4] Škorc, G., Cas, J., Brezovnik, S., Šafaric, R. (2011). Position control with parameter adaptation for a nano-robotic cell. *Strojniški vestnik - Journal of Mechanical Engineering*, vol. 57, no. 4, p. 313-322, DOI:10.5545/sv-jme.2009.017.

[5] Cheng, Y.-L., Lin, J.-H. (2007). Manufacture of three-dimensional valveless micropump. *Journal of Materials Processing Technology*, vol. 192-193, p. 229-236, DOI:10.1016/j.jmatprotec.2007.04.055.

[6] Shepard, J.F., Moses, P.J., Trolier-McKinstry, S. (1998). The wafer flexure technique for the determination of the transverse piezoelectric coefficient (d31) of PZT thin films. *Sensors and Actuators A: Physical*, vol. 71, no. 1-2, p. 133-138, DOI:10.1016/S0924-4247(98)00161-7.

[7] Guirardel, M., Bergaud, C., Cattan, E., Remiens, D., Belier, B., Petitgrand, S., Bosseboeuf, A. (2004). PZT polarization voltage effects on off-centered PZT patch actuating silicon membrane. *Sensors and Actuators A: Physical*, vol. 110, no. 3, p. 385-389, DOI:10.1016/j.sna.2003.08.016.

[8] Wong, C.W., Jeon, Y., Barbastathis, G., Kim, S.-G. (2004). Analog piezoelectric-driven gratings with nanometer resolution. *Journal of Microelectromechanical Systems*, vol. 31, no. 6, p. 998-1004, DOI:10.1109/JMEMS.2004.839592.

[9] Muralt, P., Kholkin, A., Kohli, M., Maeder, T., Setter, N. (1995). Characterization of PZT thin films for micromotors. *Microelectrical Engineering*, vol. 29, no. 1-4, p. 67-70, DOI:10.1016/0167-9317(95)00116-6.

[10] Verardi, P., Craciun, F., Dinescu, M. (1997). Characterization of PZT thin film transducers obtained by pulsed laser deposition. *Proceedings of IEEE Ultrasonics Symposium*, vol. 1, p. 569-572.

[11] Kanno, I., Kotera, H., Wasa, K. (2003). Measurement of transverse piezoelectric properties of PZT thin films. *Sensors and Actuators A: Physical*, vol. 107, no. 1, p. 68-74, DOI:10.1016/S0924-4247(03)00234-6.

[12] Huang, Z., Leighton, G., Wright, R., Duval, F., Chung. H. C., Kirby, P., Whatmore, R. W. (2007). Determination of piezoelectric coefficients and elastic constant of thin films by laser scanning vibrometry techniques. *Sensors and Actuators A: Physical*, vol. 135, no. 2, p. 660-665, DOI:10.1016/j.sna.2006.10.002.

[13] Balachandran, B., Li, H. (2003). Nonlinear phenomena in microelectromechanical resonators. *Proceedings of the IUTAM Symposium on Chaotic Dynamics and Control of Systems and Processes in Mechanics*, Rome.

[14] Li, H., Preidikman, S., Balachandran, B., Mote, Jr., C.D. (2006). Nonlinear free and forced oscillations of piezoelectric microresonators. *Journal of Micromechanics and Microengineering*, vol. 16, no. 2, p. 356-367, DOI:10.1088/0960-1317/16/2/021.

[15] Li, H., Balachandran, B. (2006). Buckling and free oscillations of composite microresonators. *Journal of Microelectromechanical Systems*, vol. 15, no. 1, p. 42-51, DOI:10.1109/JMEMS.2005.863598.

[16] Vesenjak, M., Ren, Z. (2003). Dynamic analysis of a road-restraint system's deformation resulting from a vehicle impact. *Strojniški vestnik – Journal of Mechanical Engineering*, vol. 49, no. 12, p. 586-592.

[17] DeVoe, D.L. (2001). Piezoelectric thin film micromachined beam resonators. Sensors and Actuators A: Physical, vol. 88, no. 3, p. 263-272, DOI:10.1016/S0924-4247(00)00518-5.

[18] Dick, A.J., Balachandran, B., DeVoe, D.L., Mote, Jr., C.D. (2006). Parametric identification of piezoelectric microscale resonators. *Journal of Micromechanics and Microengineering*, vol. 16, no. 8, p. 1593-1601, DOI:10.1088/0960-1317/16/8/021.

[19] Jakšić, N., Boltežar, M. (2002). Parameter identification for single-degree-of-freedom dynamic systems. *Strojniški vestnik – Journal of Mechanical Engineering*, vol. 48, no. 6, p. 302-317.

[20] Crawley, E.F., Anderson, E.H. (1990). Detailed models of piezoceramic actuation of beams. *Journal of Intelligent Materials, Systems, and Structures*, vol. 1, no. 1, p. 4-25, DOI:10.1177/1045389X9000100102.

[21] Nayfeh, A.H., Balachandran, B. (2004). *Applied Nonlinear Dynamics: Analytical, Computational, and Experimental Methods*, WILEY-VCH Verlag GmbH & Co. KGaA, Weinheim.

[22] Piekarski, B., DeVoe. D.L., Dubey, M, Kaul, R., Conrad, J. (2001). Surfaced micromachined piezoelectric resonant beam filters. *Sensors and Actuators A: Physical*, vol. 91, no. 3, p. 313-320, DOI:10.1016/S0924-4247(01)00601-X.